Generalized Fabrication of Two-Dimensional Non-Close-Packed Colloidal Crystals

Srinivasan Venkatesh and Peng Jiang*

Department of Chemical Engineering, University of Florida, Gainesville, Florida 32611

Bin Jiang

Department of Mathematics and Statistics, Portland State University, Portland, Oregon 97201

In this paper we report a generalized templating approach for fabricating wafer-scale, two-dimensional, non-close-packed (ncp) colloidal crystals. Polymer nanocomposites consisting of monolayer ncp colloidal crystals prepared by a spin-coating process are used as sacrificial templates. After removal of the colloidal silica templates, the voids in the polymer matrix are infiltrated with other materials. By plasma-etching the polymer matrix, wafer-scale ncp colloidal crystals from a variety of functional materials can be made. This technique is scalable and compatible with standard microfabrication. Two-component colloidal arrays with complex micropatterns can also be fabricated by combining microfabrication with this templating approach. Normal-incidence reflectivity spectra of replicated titania ncp arrays agree well with theoretical prediction using Scalar Wave Approximation.

Introduction

Two-dimensional (2D) ordered colloidal crystals are of considerable technological and scientific importance in nanosphere lithography,[1−3] optical devices,[4] high-density data storage,[5] biosensors,[6,7] and model systems for 2D crystallization and melting.[8] However, entropy-driven self-assembly alone is greatly restricted to the formation of close-packed crystals.[9,10] Although non-close-packed monolayer colloidal crystals are also being pursued for various nanofabrication applications, such as in fabricating nanoapertures for single quantum dot spectroscopy,[11] creating periodic nanohole arrays for surface plasmon devices,[12] making tunable superhydrophobic substrates,[13] and edge-spreading lithography,[14] current approaches based on template-induced assembly, electrostatics, optical tweezers, soft lithography, and dipole−dipole interaction suffer from low throughput and complex and expensive processes.[15−24] Additionally, only a limited number of colloids (such as silica and polymer latex) can

be routinely prepared with the narrow size distribution required for forming high-quality colloidal crystals.[9] Unfortunately, these colloids do not exhibit valuable optical, nonlinear optical, or electrooptical functionality.

To be freed from the synthetic constraints of monodisperse colloids, templating approaches have been exploited to extend the availability of functional colloidal crystals.[25−29] In general, macroporous templates are first prepared from self-assembled silica or polymer colloidal crystals. The uniform and interconnected voids of the sacrificial porous scaffolds can then be replicated into a wide variety of materials, provided the template removal process does not affect the integrity of the templated colloidal arrays. However, only close-packed colloidal crystals are used in these studies, and consequently, the replicated colloidal crystals are densely packed.[25−29] The interconnecting windows between the spherical voids in the macroporous molds are also replicated, leading to the formation of necks between neighboring spheres.[25−27] This hampers the fragmentation of colloidal assemblies into individual monodisperse particles.[30] Additionally, previous approaches typically require two steps in forming macroporous hosts, involving the production of colloidal crystal templates and the subsequent replication step. These processes are tedious in making large-area (centimeter-scale) samples and are not compatible with standard wafer-scale batch microfab-

* To whom correspondence should be addressed. E-mail: pjiang@che.ufl.edu.

(1) Deckman, H. W.; Dunsmuir, J. H. *Appl. Phys. Lett.* **1982**, *41*, 377.
(2) Haynes, C. L.; Van Duyne, R. P. *J. Phys. Chem. B* **2001**, *105*, 5599.
(3) Choi, D. G.; Yu, H. K.; Jang, S. G.; Yang, S. M. *J. Am. Chem. Soc.* **2004**, *126*, 7019.
(4) Mafouana, R.; Rehspringer, J. L.; Hirlimann, C.; Estournes, C.; Dorkenoo, K. D. *Appl. Phys. Lett.* **2004**, *85*, 4278.
(5) Sun, S. H.; Murray, C. B.; Weller, D.; Folks, L.; Moser, A. *Science* **2000**, *287*, 1989.
(6) Baksh, M. M.; Jaros, M.; Groves, J. T. *Nature* **2004**, *427*, 139.
(7) Velev, O. D.; Kaler, E. W. *Langmuir* **1999**, *15*, 3693.
(8) Eisenmann, C.; Gasser, U.; Keim, P.; Maret, G. *Phys. Rev. Lett.* **2004**, *93*, 105702.
(9) Xia, Y. N.; Gates, B.; Yin, Y. D.; Lu, Y. *Adv. Mater.* **2000**, *12*, 693.
(10) Pieranski, P. *Contemp. Phys.* **1983**, *24*, 25.
(11) Hakanson, U.; Persson, J.; Persson, F.; Svensson, H.; Montelius, L.; Johansson, M. K. J. *Nanotechnology* **2003**, *14*, 675.
(12) Jiang, P. *Angew. Chem., Int. Ed.* **2004**, *43*, 5625.
(13) Han, J. T.; Lee, D. H.; Ryu, C. Y.; Cho, K. *J. Am. Chem. Soc.* **2004**, *126*, 4796.
(14) McLellan, J. M.; Geissler, M.; Xia, Y. N. *J. Am. Chem. Soc.* **2004**, *126*, 10830.
(15) Grier, D. G. *Nature* **2003**, *424*, 810.
(16) Lumsdon, S. O.; Kaler, E. W.; Velev, O. D. *Langmuir* **2004**, *20*, 2108.
(17) Ristenpart, W. D.; Aksay, I. A.; Saville, D. A. *Phys. Rev. Lett.* **2003**, *90*, 128303.
(18) van Blaaderen, A.; Ruel, R.; Wiltzius, P. *Nature* **1997**, *385*, 321.

(19) Yin, Y. D.; Lu, Y.; Gates, B.; Xia, Y. N. *J. Am. Chem. Soc.* **2001**, *123*, 8718.
(20) Hoogenboom, J. P.; Retif, C.; de Bres, E.; de Boer, M. V.; van Langen-Suurling, A. K.; Romijn, J.; van Blaaderen, A. *Nano Lett.* **2004**, *4*, 205.
(21) Aizenberg, J.; Braun, P. V.; Wiltzius, P. *Phys. Rev. Lett.* **2000**, *84*, 2997.
(22) Yan, X.; Yao, J. M.; Lu, G.; Li, X.; Zhang, J. H.; Han, K.; Yang, B. *J. Am. Chem. Soc.* **2005**, *127*, 7688.
(23) Tan, B. J. Y.; Sow, C. H.; Lim, K. Y.; Cheong, F. C.; Chong, G. L.; Wee, A. T. S.; Ong, C. K. *J. Phys. Chem. B* **2004**, *108*, 18575.
(24) Zheng, H. P.; Rubner, M. F.; Hammond, P. T. *Langmuir* **2002**, *18*, 4505.
(25) Yang, S. M.; Coombs, N.; Ozin, G. A. *Adv. Mater.* **2000**, *12*, 1940.
(26) Jiang, P.; Bertone, J. F.; Colvin, V. L. *Science* **2001**, *291*, 453.
(27) Johnson, S. A.; Ollivier, P. J.; Mallouk, T. E. *Science* **1999**, *283*, 963.
(28) Xu, L. B.; Tung, L. D.; Spinu, L.; Zakhidov, A. A.; Baughman, R. H.; Wiley, J. B. *Adv. Mater.* **2003**, *15*, 1562.
(29) Yi, G. R.; Moon, J. H.; Manoharan, V. N.; Pine, D. J.; Yang, S. M. *J. Am. Chem. Soc.* **2002**, *124*, 13354.
(30) Zhong, Z. Y.; Yin, Y. D.; Gates, B.; Xia, Y. N. *Adv. Mater.* **2000**, *12*, 206.

rication, impeding their scalability and practical applications. Finally, only single-component colloidal crystals have been made by early approaches.[25−29] The interconnecting windows between the spherical voids prevent selective infiltration of specific voids to form multicomponent colloidal arrays that might find important applications in microoptics and sensors.[31]

To resolve the scalability and compatibility issues of current self-assemblies, we have recently developed a robust spin-coating technique for assembling ncp colloidal crystals.[32,33] The methodology is based on shear-aligning concentrated colloidal suspensions using standard spin-coating equipment. The technique is simple and compatible with standard microfabrication, enabling reproducible fabrication of wafer-scale, non-close-packed crystals with thickness ranging from a monolayer to hundreds of layers.[32,33] Unfortunately, only monodisperse silica particles can be used in the process and the extension of the spin-coating technique to other functional materials is mainly restricted by the availability of highly uniform colloidal particles. We have also demonstrated that spin-coated ncp colloidal arrays can be used as structural templates to replicate a myriad of nanostructures. For instance, metallic nanohole arrays have been replicated from monolayer ncp colloidal arrays by masked deposition and particle lift-off.[34] The modulated surface features of three-dimensional (3D) ncp colloidal crystals have been demonstrated as 2D templates to create wafer-scale surface gratings.[12] 3D macroporous polymers[32] and 2D attoliter polymer microvial and microwell arrays[35,36] have been templated from shear-aligned nanocomposites. The templated polymer microwell arrays can again be used as lift-off masks to fabricate magnetic nanodot arrays over a large area.[36]

Here we extend our previous work on templated macroporous polymers and microvial arrays[32,35,36] to develop a generalized templating approach for fabricating wafer-scale ncp colloidal crystals from a variety of functional materials. Monolayer, ncp colloidal crystals have been replicated inside the cavities of a macroporous polymer film which itself is a replica of a spin-coated ncp silica colloidal crystal.[32] Significantly distinguished from our previous work on templated nanofabrication, where planar and circular nanostructures (e.g., nanoholes) are replicated against spherical particles, the templated colloidal arrays in this work retain the spherical shapes of the original silica templates. Contrary to conventional self-assemblies, silica spheres in the spin-coated colloidal arrays are not connected, eliminating the interconnecting windows in the macroporous templates.[35] Thus, the resulting replicated colloids are well separated from each other and no posttreatment is required to break the necks between neighboring spheres to make monodisperse colloids. Most important, the technique is scalable and two-component colloidal arrays with complex micropatterns can be created by standard microfabrication. The optical properties of replicated titania ncp arrays agree well with theoretical prediction using Scalar Wave Approximation (SWA).

Experimental Section

Materials and Substrates. All solvents and chemicals are of reagent quality and are used without further purification. Ethanol (200-proof) is obtained from Pharmaco Products. Technical-grade hydrofluoric acid (49%), titanium isopropoxide, zirconium butoxide, aluminum *sec*-butoxide, 2-propanol, 1-butanol, and 2-butanol are

purchased from Sigma-Aldrich. Ultrapure water (18.2 MΩ cm^{-1}) is used directly from a Barnstead water system. Monodispersed silica colloids with less than 5% diameter variation are synthesized by the Stober method.[37,38] Ethoxylated trimethylolpropane triacrylate (ETPTA) monomer is obtained from Sartomer (Exton, PA). The photoinitiator Darocur 1173 (2-hydroxy-2-methyl-1-phenyl-1-propanone) is provided by Ciba Specialty Chemicals. The silicon wafer primer (3-acryloxypropyl)trichlorosilane (APTCS) is purchased from Gelest (Morrisville, PA). Silicon wafers (test grade, n type, (100)) are obtained from Wafernet (San Jose, CA) and are primed by swabbing APTCS on the wafer surfaces using clean room Q-tips (Fisher), rinsed with 200-proof ethanol twice, and baked on a hot plate at 110 °C for 2 min.

Instrumentation. Scanning electron microscopy (SEM) and energy-dispersive X-ray (EDX) analysis are carried out on a JEOL 6335F FEG-SEM instrument. Powder X-ray diffraction (XRD) is performed on a Philips APD 3720 system. A standard spin-coater (WS-400B-6NPP-Lite spin processor, Laurell) is used to spin-coat colloidal suspensions. The polymerization of ETPTA monomers is carried out on a pulsed UV curing system (RC 742, Xenon). A Plasma-Therm 790 reactive ion etcher (Unaxis) is utilized to partially remove polymerized ETPTA for making macroporous polymer membranes. Photolithography is carried out on a Karl Suss MA6 mask aligner.

Preparation of Macroporous Polymer Membranes. The fabrication of wafer-scale, monolayer, non-close-packed colloidal crystal−polymer nanocomposites is performed according to ref 33. In short, monodispersed silica colloids are dispersed in ETPTA to make a final particle volume fraction of ∼20%. Darocur 1173 (2% by weight) is added as the photoinitiator. The silica−ETPTA dispersion is dispensed on an APTCS-primed (100) silicon wafer and spin-coated at 8000 rpm for 6 min on a standard spin-coater, yielding a hexagonally ordered colloidal monolayer. The monomer is then photopolymerized for 4 s using a pulsed UV curing system. The polymer matrix is partially removed using a reactive ion etcher operating at a 40 mTorr oxygen pressure, a 100 sccm flow rate, and 100 W for 15 s. A hydrofluoric acid aqueous solution (2%) is then utilized to dissolve silica templating colloids. The removal of the templating silica particles creates a visible color change during wet etching.

Templated Fabrication of Monolayer Colloidal Crystals. To fill the cavities of the macroporous films, we first dip the wafer-supported membranes in an alcoholic solution of metal alkoxide. For making titania colloidal crystals, we use 30 vol % titanium(IV) isopropoxide in 2-praponol as the ceramic precursor, while, for zirconia and alumina, 30 vol % zirconium butoxide and aluminum *sec*-butoxide in their corresponding alcohols are used. After infiltration in the precursor solution for about 1 h, the wafer is removed and dipped into water for 1 min. Metal oxide coatings on the outer surface of the wafer are washed away by gently rubbing the sample using a clean room Q-tip. To completely fill the voids, 8−12 cycles of infiltration and reaction are performed. The polymer matrix can then be removed by plasma etching operating at a 40 mTorr oxygen pressure, a 100 sccm flow rate, and 100 W for 2 min.

Photolithographic Patterning of Monolayer Colloidal Crystals and Fabrication of Patterned Two-Component Monolayer Colloidal Arrays. For photolithographic patterning, a 1.5 μm thick Shipley 1813 photoresist is spin-coated onto the polymerized silica−ETPTA nanocomposite. The photoresist is then photolithographically patterned to open etching windows. A Plasma-Therm 790 reactive ion etcher operating at the same conditions as described above is utilized to completely remove the polymer matrix underneath the etching windows. After removal of the photoresist by acetone wash and the exposed silica spheres by a clean room Q-tip under flowing water, oxygen plasma etching is used again to expose silica spheres with specific microstructures. To make micropatterned two-component monolayer colloidal arrays, the same photolithographic

(31) Li, H. L.; Dong, W. T.; Bongard, H. J.; Marlow, F. *J. Phys. Chem. B* **2005**, *109*, 9939.

(32) Jiang, P.; McFarland, M. J. *J. Am. Chem. Soc.* **2004**, *126*, 13778.

(33) Jiang, P.; Prasad, T.; McFarland, M. J.; Colvin, V. L. *Appl. Phys. Lett.* **2006**, *89*, 011908.

(34) Jiang, P.; McFarland, M. J. *J. Am. Chem. Soc.* **2005**, *127*, 3710.

(35) Jiang, P. *Chem. Commun.* **2005**, 1699.

(36) Jiang, P. *Langmuir* **2006**, *22*, 3955.

(37) Stober, W.; Fink, A.; Bohn, E. *J. Colloid Interface Sci.* **1968**, *26*, 62.

(38) Jiang, P.; Bertone, J. F.; Hwang, K. S.; Colvin, V. L. *Chem. Mater.* **1999**, *11*, 2132.
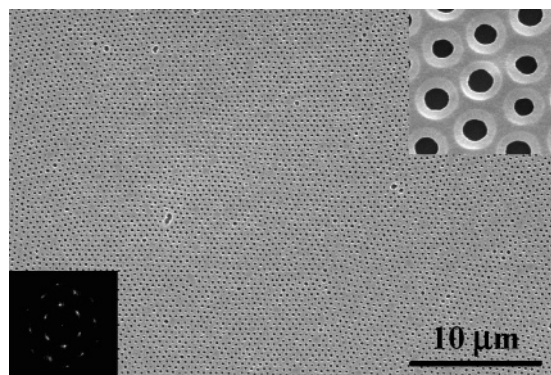
Figure 1. Typical SEM image of a macroporous polymer with 2D crystalline arrays of voids templated from a non-close-packed silica colloidal crystal−polymer nanocomposite prepared by spin-coating. The top inset shows a magnified SEM image, and the bottom inset shows a Fourier transform of a 40×40 μm region.

patterning process is performed. Instead of complete removal, the exposed polymer membranes underneath the etching windows are only partially removed by RIE (15 s etching at the above conditions). After the silica spheres are dissolved in a 2% hydrofluoric acid aqueous solution, the photoresist layer is washed away by acetone. The voids are then filled by metal oxides, followed by complete RIE etching of the polymer matrix using the above RIE receipts.

Normal-Incidence Optical Reflectivity Measurements. An Ocean Optics HR4000 high-resolution fiber optic UV−vis−near-IR spectrometer with a reflection probe is used for reflectance measurements. A calibrated halogen light source is used to illuminate the sample, and the spectrometer can scan wavelengths from 350 to 1100 nm. The beam spot size is about 3 mm on the sample surface. Measurements are performed at normal incidence, and the cone angle of collection is less than 5°. Absolute reflectivity is obtained as the ratio of the sample spectrum and the reference spectrum. The reference spectrum is the optical density obtained from an aluminum-sputtered (1000 nm thickness) silicon wafer. The final value of the absolute reflectivity is the average of several measurements obtained from different spots on the sample surface.

SWA Optical Simulation. The SWA calculation[33,39] is performed to predict the optical reflectance from the colloidal monolayer. In SWA model, two assumptions are made to simplify the calculation of electromagnetic propagation in periodic dielectric media.[39] The first is that the electric field is treated as a scalar rather than a vector quantity. The second is that scattering off of all except the {111} lattice plane of a face-centered cubit (fcc) crystal is neglected. For SWA calculation of a monolayer titania colloidal crystal, the lattice spacing is set to ($\sqrt{2}$)D (D is the diameter of the templated titania particles) and a refractive index of 2 is used for amorphous titania.[40]

Results and Discussion

We use the spin-coating technique[33,34] to fabricate 2D colloidal crystal−polymer nanocomposites as the starting template. Dispersions of monodisperse silica particles in ETPTA are spin-coated onto silicon wafers and subsequently photopolymerized to create ncp colloidal arrays. The shear-aligned particles are embedded in a polymer matrix with an interparticle distance around ($\sqrt{2}$)D, where D is the diameter of the silica spheres.[33] A reactive ion etcher is used to partially remove the polymer matrix. A hydrofluoric acid aqueous solution (2%) is then utilized to dissolve the silica templating colloids, leaving behind a wafer-scale macroporous polymer film supported by the substrate. Figure 1 shows a typical SEM image of a resulting macroporous polymer film templated from 325 nm silica spheres. The long-range
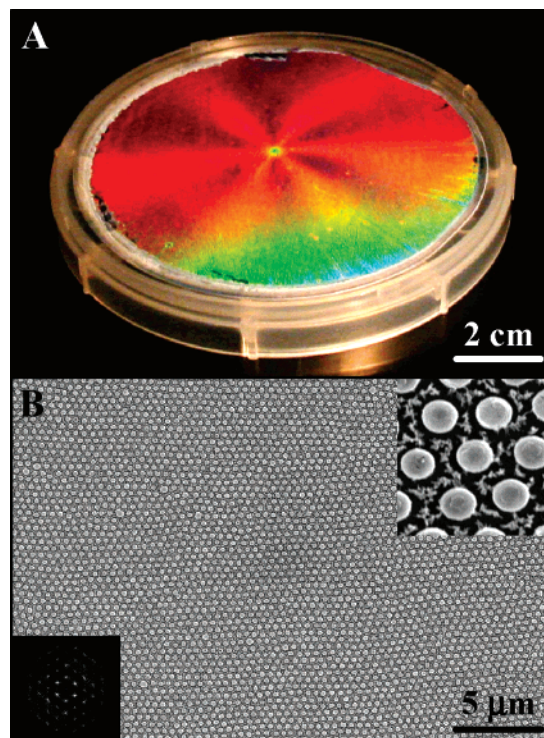
(39) Satpathy, S.; Zhang, Z.; Salehpour, M. R. *Phys. Rev. Lett.* **1990**, *64*, 1239.
(40) Rengarajan, R.; Jiang, P.; Colvin, V.; Mittleman, D. *Appl. Phys. Lett.* **2000**, *77*, 3517.

Figure 2. Templated wafer-scale titania monolayer ncp colloidal crystal: (A) photograph of a sample on a 4 in. silicon wafer illuminated with white light, (B) typical SEM image of the sample shown in (A). The top inset shows a magnified SEM image, and the bottom inset shows a Fourier transform.
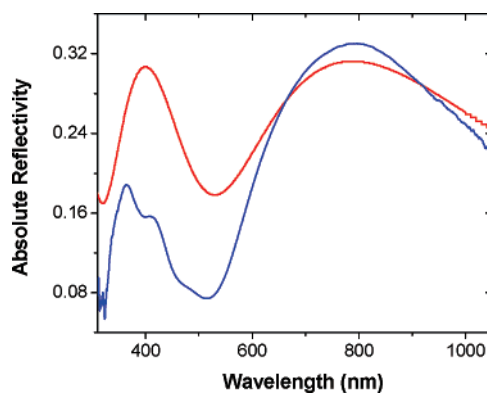

Figure 3. Normal-incidence reflectivity spectrum (blue curve) of the sample shown in Figure 2A. The red curve is calculated using SWA by assuming the refractive index of amorphous titania to be 2.

hexagonal ordering of voids is apparent from the SEM image and its Fourier transform (FFT) shown in the bottom inset of Figure 1. To confirm the complete removal of silica colloids, the macroporous polymer films are thoroughly plasma-etched, and no residue is found on the substrate. From the magnified SEM images as shown in the top inset of Figure 1, the center-to-center distance between neighboring voids is determined to be 463 $\pm$ 10 nm, which is $\sim$1.4 times of the diameter of the templating silica spheres ($\sim$325 nm), indicating the preservation of the original ncp arrangement of silica particles in the macroporous polymer replica.[32,33]

We then use the well-known metal alkoxide sol−gel chemistry to fill the spherical voids of the macroporous polymer hosts.[41]

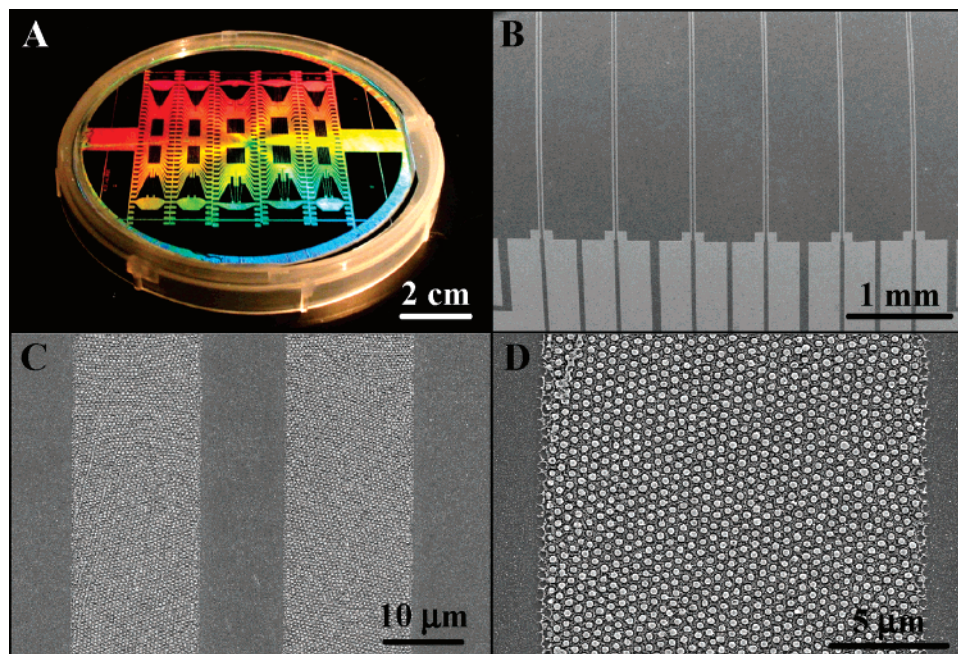(41) Holland, B. T.; Blanford, C. F.; Stein, A. *Science* **1998**, *281*, 538.

Figure 4. Micropatterned zirconia monolayer ncp colloidal crystal: (A) photograph of a 4 in. sample under white light, (B) low-magnification SEM image, (C) typical SEM image of a double-line pattern shown in (B), (D) magnified SEM image of a portion of the double line in (C).

The wafer-supported macroporous film is first immersed in an alcoholic solution of metal alkoxide; once the film is removed and dipped into water, the alkoxides, which fill the cavities, hydrolyze and condense to form metal oxides. Through successive deposition, the voids can be completely filled. The polymer hosts are then removed by oxygen plasma etching, leaving behind monolayer ncp colloidal crystals that retain the initial silica template geometry. Figure 2A shows a photograph of a 4 in. diameter titania ncp colloidal crystal templated from 325 nm silica spheres by using titanium(IV) isopropoxide as the ceramic precursor. The long-range hexagonal ncp arrangement of the templated titania colloidal crystal is confirmed by the SEM image and its Fourier transform in Figure 2B and its bottom inset. The periodic particle arrays function as a 2D diffraction grating, causing the striking colors shown in Figure 2A. The size of the replicated particles is measured to be 305 ± 17 nm, which is slightly smaller than that of the initial silica spheres (325 nm), while the center-to-center distance between adjacent spheres is the same as that of the macroporous hosts. The chemical compositions of the replicated particles are determined by EDX analysis to contain ~42 wt % titanium and ~40 wt % oxygen. No silicon element is detected by EDX. Powder XRD results show the templated titania particles are amorphous. From the magnified SEM image in the upper inset of Figure 2B, branched titania agglomerates are found surrounding uniform titania particles. They arise from the nonspecific deposition of sol−gel titania on the macroporous polymer surface. Brief etching in diluted acid prior to the removal of the polymer host could help to eliminate unwanted material deposition on the outer polymer surface.

The optical properties of the templated titania ncp colloidal crystals are evaluated using a vis−near-IR reflectivity measurement at normal incidence and an SWA calculation.[39,42] For a colloidal photonic crystal, we know that, as the thickness of the film increases, the peak height increases and the peak width decreases.[42] Here we are going to take the reflectivity spectrum

of a very thin film: it has only one layer. It is expected that it will have a broad peak with a small peak height. This is exactly what we observe in optical measurements. Figure 3 shows the comparison between the reflectivity spectrum of a 305 nm diameter titania sample as shown in Figure 2 and the calculated spectrum for a sample with a lattice parameter of $(\sqrt{2})D$. The shapes and positions of two reflection peaks centered around 400 and 800 nm and the absolute reflectivity of the main peak (795 nm) of the experimental spectrum match those of the SWA calculation, but the height of the secondary peak around 400 nm is lower than the theoretical prediction. The branched agglomerates surrounding uniform titania particles (upper inset of Figure 2B) and the polycrystalline characteristic of the monolayer array, as well as the surface roughness of the templated titania particles, could give rise to the mismatch. The standard deviation of the absolute reflectivity at the main peak is determined to be ~5.3% by averaging 40 measurements across the 4 in. sample shown in Figure 2A, indicating uniform coverage of ncp colloidal arrays over a large area.

Besides providing a versatile technique for fabricating ncp colloidal crystals from a variety of functional materials, another major merit of this technique is in its compatibility with conventional microfabrication. Standard photolithography and oxygen plasma etching are utilized to create wafer-scale ncp zirconia colloidal crystals with complex micropatterns as shown in Figure 4A. The sample exhibits bright six-arm diffraction under white light illumination and has well-defined features shown by the images in Figure 4B,C. The micropatterned colloidal array retains the size and the center-to-center distance of the spherical voids in the macroporous polymer evidenced by the magnified image in Figure 4D.

In sharp contrast to conventional macroporous polymers templated from close-packed colloidal crystals,[25−27,29] the voids in the spin-coating-based porous films are isolated from each other.[35] This enables the selective infiltration of specific voids to form two-component ncp colloidal arrays with well-defined microfeatures by combining standard microfabrication with the current templating strategy. A photolithographically

(42) Bertone, J. F.; Jiang, P.; Hwang, K. S.; Mittleman, D. M.; Colvin, V. L. *Phys. Rev. Lett.* **1999**, *83*, 300.
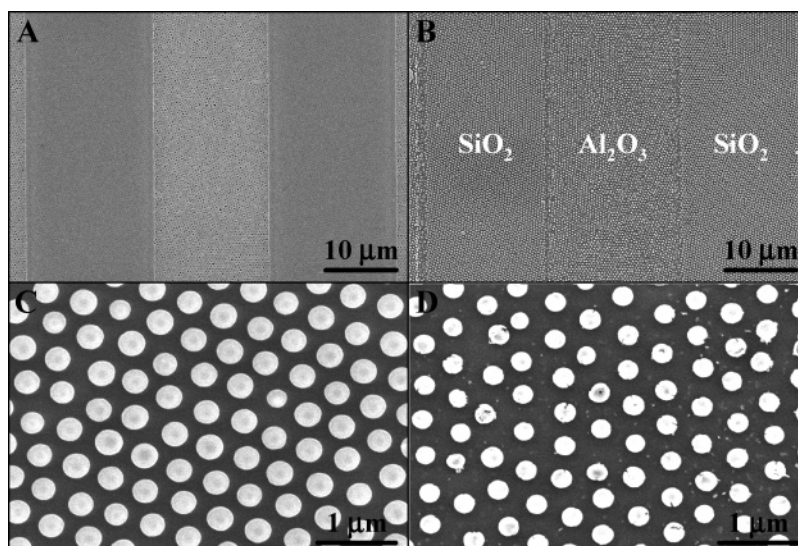
Figure 5. Micropatterned two-component ncp colloidal arrays: (A) top-view SEM image of a micropatterned template with periodic stripes of the nanocomposites and macroporous host, (B) SEM image of patterned silica and alumina colloidal stripes, (C) magnified SEM image of colloidal silica arrays in (B), (D) magnified SEM image of colloidal alumina arrays in (B).

defined photoresist is utilized to protect the underlying polymer matrix against a brief oxygen plasma etching. The partially exposed silica spheres can be etched away, while the protected silica particles under photoresist patterns remain intact due to the non-close-packing of the colloidal templates. Figure 5A shows a micropatterned film with a periodic arrangement of stripes of the nanocomposites and macroporous host. After infiltration of the spherical voids with a functional material, followed by oxygen plasma etching to remove the polymer matrix, a micropatterned binary colloidal array can be made. Figure 5B illustrates patterned binary colloidal arrays consisting of silica and alumina stripes. The non-close-packed hexagonal arrangement of silica and alumina particles is clearly evident from the magnified SEM images shown in Figure 5C,D. However, due to the incomplete filling of spherical voids (six infiltration/ reaction cycles), the resulting alumina particles (297 nm diameter) are significantly smaller than the templating silica particles (370 nm). The unwanted material deposition between templated particles (see Figures 2B and 4D) is avoided due to the weak adhesion of sol−gel alumina on the outer polymer surface.

Conclusions

In conclusion, we have developed a generalized templating approach for fabricating wafer-scale ncp colloidal crystals from a variety of functional materials, without developing synthetic methods for highly uniform colloids of each material. Although only alkoxide-derived metal oxides are demonstrated here, the templating technique can be easily extended to other functional materials, such as metals and semiconductors,[25−29] provided they sustain oxygen plasma etching during polymer host removal. This technique is compatible with standard semiconductor microfabrication and enables the creation of two-component colloidal arrays with complex micropatterns. The normal-incidence reflectivity spectra of the templated colloidal mono-layers match the theoretical prediction using SWA. The resulting 2D ncp colloidal arrays may find important technological applications ranging from microoptics to nanofabrication.